university of groningen

University Medical Center Groningen

University of Groningen

High-resolution dimethyl sulfide and dimethylsulfoniopropionate time series profiles in decaying summer first-year sea ice at Ice Station Polarstern, western Weddell Sea, Antarctica

Tison, J. -L.; Brabant, F.; Dumont, I.; Stefels, J.

Published in:
Journal of geophysical research-Biogeosciences

DOI:
10.1029/2010JG001427

IMPORTANT NOTE: You are advised to consult the publisher's version (publisher's PDF) if you wish to cite from it. Please check the document version below.

Document Version
Publisher's PDF, also known as Version of record

Publication date:
2010

Link to publication in University of Groningen/UMCG research database

Citation for published version (APA):
Tison, J. -L., Brabant, F., Dumont, I., & Stefels, J. (2010). High-resolution dimethyl sulfide and dimethylsulfoniopropionate time series profiles in decaying summer first-year sea ice at Ice Station Polarstern, western Weddell Sea, Antarctica. *Journal of geophysical research-Biogeosciences*, *115*. https://doi.org/10.1029/2010JG001427

Copyright
Other than for strictly personal use, it is not permitted to download or to forward/distribute the text or part of it without the consent of the author(s) and/or copyright holder(s), unless the work is under an open content license (like Creative Commons).

The publication may also be distributed here under the terms of Article 25fa of the Dutch Copyright Act, indicated by the “Taverne” license. More information can be found on the University of Groningen website: https://www.rug.nl/library/open-access/self-archiving-pure/taverne-amendment.

Take-down policy
If you believe that this document breaches copyright please contact us providing details, and we will remove access to the work immediately and investigate your claim.

Downloaded from the University of Groningen/UMCG research database (Pure): http://www.rug.nl/research/portal. For technical reasons the number of authors shown on this cover page is limited to 10 maximum.

High-resolution dimethyl sulfide and dimethylsulfoniopropionate time series profiles in decaying summer first-year sea ice at Ice Station Polarstern, western Weddell Sea, Antarctica

J.-L. Tison,[1] F. Brabant,[1] I. Dumont,[2] and J. Stefels[3]

Received 13 May 2010; revised 1 September 2010; accepted 20 September 2010; published 31 December 2010.

[1] High-resolution profiles of ice dimethyl sulfide (DMS) and dimethylsulfoniopropionate (DMSP) concentrations were measured together with a suite of ancillary physical and biological properties during a time series of decaying summer-level first-year sea ice throughout December 2004 during the Ice Station Polarstern drift experiment (western Weddell Sea, Antarctica). Ice DMSP and DMS concentrations were always maximum at the bottom of the ice sheet (636–2627 and 292–1430 n*M*, respectively) where the highest chlorophyll *a* levels were also found (15–30 μg L^{-1}). Throughout the observation period, the autotrophic surface community (32–205 μg C L^{-1}) was dominated by *Phaeocystis* sp. while the bottom community (1622–3830 μg C L^{-1}) mainly consisted of pennate diatoms. This illustrates that, although being known for lower DMSP-to-chlorophyll *a* ratios than *Phaeocystis* sp., diatoms dominated the overall DMSP production because of their much larger biomass. Decreasing DMSP concentrations and increasing DMS-to-DMSP ratios in the bottom layers with time suggested active DMSP-to-DMS conversion in a slowly degrading environment. Drastic temporal brine volume and brine salinity changes associated with the decaying sea ice cover are shown to directly impact (1) the migration of DMSP and DMS through the brine network, (2) the DMSP-to-DMS conversion processes within the ice interior, and (3) the physiological response of the ice algae. First-order flux estimates show that decaying summer-level first-year sea ice alone can significantly contribute to the regional sulfur budget of the Weddell Sea with an estimated average loss rate of 5.7 μmol DMS(P) m^{-2} d^{-1}) toward the atmosphere and the ocean.

Citation: Tison, J.-L., F. Brabant, I. Dumont, and J. Stefels (2010), High-resolution dimethyl sulfide and dimethylsulfoniopropionate time series profiles in decaying summer first-year sea ice at Ice Station Polarstern, western Weddell Sea, Antarctica, *J. Geophys. Res.*, *115*, G04044, doi:10.1029/2010JG001427.

1. Introduction

[2] Dimethyl sulfide (DMS) is a biogenic semivolatile organic compound mainly produced by the enzymatic conversion of dimethylsulfoniopropionate (DMSP). DMSP is synthesized by a limited number of phytoplanktonic taxa in oceanic environments [*Keller et al.*, 1989]. A complex ecosystem network that involves most of the microbial food web affects the concentrations of DMS and DMSP in the environment, resulting in strong seasonal and latitudinal variations in concentration in surface ocean waters (reviewed by *Stefels et al.* [2007]). DMS accounts for 50% to 60% of Earth's total natural sulfur emissions to the atmosphere, and 90% of this DMS flux originates in marine environments. DMS has been brought forward to the scene of climate change as a potential mitigation agent of global warming from increasing concentrations of greenhouse gases. Indeed, once released in the atmosphere, DMS is oxidized to, among other compounds, sulfate that can either directly (as aerosols) or indirectly (as cloud condensation nuclei) increase the reflectivity of the atmosphere and of the clouds, thereby cooling the Earth. *Charlson et al.* [1987] suggested that the temperature increase resulting from global warming would raise biogenic production of DMS that would in turn increase the rate of formation of sulfate aerosols, thereby impeding the temperature increase, at least partially. This assumption is challenged by the observation that not all microalgae are able to synthesize DMSP and that the effect of climate change on the growth of DMSP producers is not known because of a lack of understanding of the factors controlling DMSP variability in phytoplankton cells as well as those factors acting on DMSP-to-DMS

[1] Laboratoire de Glaciologie, Faculté des Sciences, Université Libre de Bruxelles, Brussels, Belgium.
[2] Ecologie des Systèmes Aquatiques, Faculté des Sciences, Université Libre de Bruxelles, Brussels, Belgium.
[3] Laboratory of Plant Physiology, University of Groningen, Haren, Netherlands.

Copyright 2010 by the American Geophysical Union.
0148-0227/10/2010JG001427

Table 1. Summary of Available Sea Ice DMS and DMSP Data in the Literature

Location	Ice Type	Season[a]	DMSP[b] (n*M*)	DMS[b] (n*M*)	DMS+DMSP[b] (n*M*)	Source
Weddell Sea	Pack ice	Sp	**322** (4–1664)	NA	NA	*Kirst et al.* [1991]
Resolute Passage	Pack ice	Sp	**325**[c] (0–6014)[c]	NA	**950**[d] (nd–15051)[d]	*Levasseur et al.* [1994]
Bellingshausen Sea	Pack ice	Sp-Su	**200** (17–546)	NA	NA	*Turner et al.* [1995]
Prydz Bay	Pack ice	Sp	**144** (8–725)	NA	NA	*Curran et al.* [2003]
Dumont D'Urville Sea	Pack ice	Wi	**40** (nd-193)	NA	NA	*Curran et al.* [2003]
Ross Sea	Pack ice	Sp-Su	**212** (5–980)	NA	NA	*DiTullio et al.* [1998]
Ross Sea	Fast ice	Sp	**150** (81–219)	NA	NA	*DiTullio et al.* [1998]
Offshore Prydz Bay	Pack ice	Sp	**107** (6–787)	NA	NA	*Trevena et al.* [2003]
Baffin Bay	Pack ice	Sp-Su	**126**[c] (8.66–987)[c]	NA	NA	*Lee et al.* [2001]
Prydz Bay	Fast ice	Sp-Su	**112** (9–1478)	NA	NA	*Trevena et al.* [2003]
Gerlache Inlet	Fast ice	Su	**NA** (4.4–450)	NA	NA	*Gambaro et al.* [2004]
Indian sector of SO	Pack/fast ice	Sp	**185**[e,f] (45–796)[e]	**12** (<0.3–75)	NA	*Trevena and Jones* [2006]
Dumont D'Urville Sea	Fast ice	Sp	NA	**NA** (4–74)	NA	*Delille et al.* [2007]
Western Weddell Sea	Pack ice	Summer	**171** (5–2627)	**58** (0.5–1430)	**229** (6–3340)	This study

[a]Sp, spring; Su, summer; Wi, winter; NA, not available; SO, Southern Ocean.
[b]Mean is given in bold, followed by the range in parentheses.
[c]$DMSP_p$ only.
[d]$DMSP_d$ + DMS.
[e]Calculated for ice categories with ice thickness <1.20 m.
[f]Number of cores weighted average.

transformation. Among the unknowns, processes in sea ice form the biggest gap in our knowledge, even though sea ice is known to be a habitat for strong DMSP-producing algal species [*Kirst et al.*, 1991; *Levasseur et al.*, 1994]. Another potential by-product of the marine DMS released to the atmosphere, which is also of climatic significance, is methylsulfonic acid, which is found in continental ice cores and often used as a paleoclimatic indicator of regional sea ice extent, at least in coastal areas [*Mulvaney et al.*, 1992; *Welch et al.*, 1993; *Pasteur et al.*, 1995; *Meyerson et al.*, 2002; *Curran et al.*, 2003; *Wolff et al.*, 2006; *Abram et al.*, 2007; *Rhodes et al.*, 2009].

[3] Suggested biological functions for DMSP are an osmotic pressure regulator, a cryoprotectant, an oxygen radical scavenger, an overflow compound for excess energy dissipation, and a grazing deterrent. Although DMSP seems to be a multifunctional compound, the regulation of its production and conversion is still unresolved. Several environmental factors such as salinity, light intensity and history, temperature, and nutrient supply may affect the DMSP synthesis by algal cells (reviewed by *Stefels* [2000] and *Stefels et al.* [2007]). Unlike the relatively stable pelagic environment, sea ice forms a habitat where extremely high salinities and low temperatures favor the enhanced production of DMSP in algal cells. Subsequent melting of ice results in very low salinities and higher temperatures, which mediates the release of DMSP from cells and increases the conversion to DMS. During springtime, light conditions at the ice surface may become inhibiting. Under such conditions, an increased DMSP production is expected, although the mechanisms are still enigmatic. Moreover, in field samples, the multitude of processes are difficult to follow separately and the overarching effect of high light conditions may be the inhibited conversion of DMS and DMSP by bacteria and an increased photochemical conversion of DMS to dimethylsulfoxide (DMSO) [*Slezak et al.*, 2001]. Release of DMSP from algal cells is mediated by active exudation, cell lysis due to senescence or viral attack, or grazing. The conversion of DMSP into DMS and acrylic acid is mainly mediated through bacterial or algal enzymes; however, in sea ice, chemical conversion should be considered as well. Hydroxide decomposition of DMSP does not take place at the pH of seawater, but the potentially alkaline conditions of sea ice brine inclusions, with pH values sometimes rising as high as 10 [*Gleitz et al.*, 1995], do favor abiotic conversion. Whether these alkaline conditions also favor the enzymatic conversion of DMSP is unknown. Although it was observed that the pH optimum of DMSP lyase in a temperate *Phaeocystis* species was indeed alkaline [*Stefels and Dijkhuizen*, 1996], various strains of *Emiliania huxleyi*, another Haptophyte species, indicated the existence of various isoforms of DMSP lyase that have different pH optima [*Steinke et al.*, 1998]. There is nothing known about DMSP lyase activity and its characteristics in ice algae. To date, sea ice DMSP and DMS studies were mainly focused on DMSP (Table 1), and only two of these studies report individual DMS concentrations. Even though they are scarce, published values confirm the assumption of sea ice as an environment favorable to DMSP and DMS production, with concentration levels up to three orders of magnitude higher than background (subnanomolar) values in seawater [e.g., *Kirst et al.*, 1991; *Turner et al.*, 1995; *DiTullio et al.*, 1998]. This paper presents the first high-resolution DMS and DMSP time series profiles in the level spring/summer first-year sea ice of 2004 at the ISPOL "clean site" [*Tison et al.*, 2008] in the western Weddell Sea and discusses how these profiles are related to the decay processes of the ice. More specifically, we focus on deciphering the relative contribution and potential interactions between physical and biological processes in controlling the DMS(P) cycle within the sea ice and we provide first estimates of the sulfur fluxes to the ocean and the atmosphere from summer sea ice in the western Weddell Sea.

2. Site Description

[4] DMS and DMSP measurements were obtained from samples collected at the ISPOL clean site, which was described extensively by *Tison et al.* [2008]. Briefly, ice cores, brines, and under ice water samples were collected at regular 5 day intervals from 29 November to 30 December

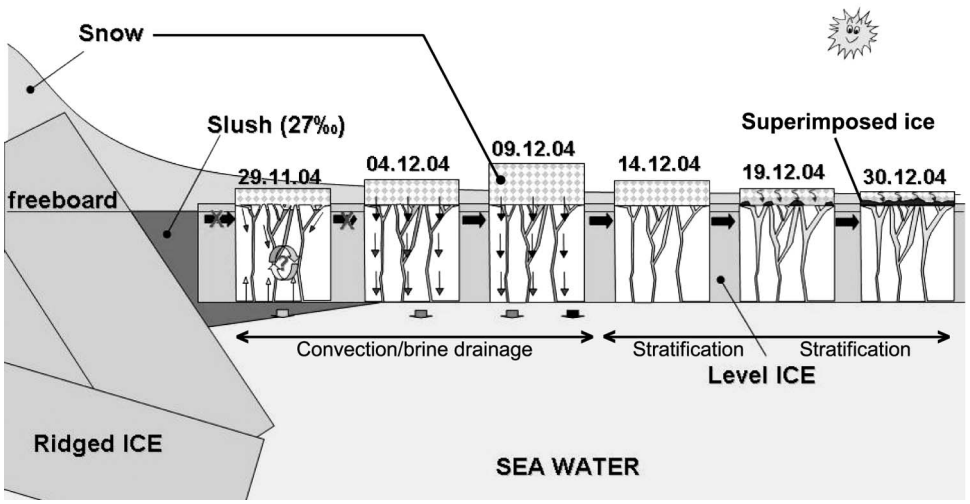

Figure 1. Schematic evolution of the decaying first-year sea ice cover at the ISPOL clean site [after *Tison et al.*, 2008]. Vertical arrows indicate brine drainage in the first half of the observation period. Horizontal arrows indicate lateral brine movement. Station 25 December is similar to 30 December (30.12.04) and is not shown. Note that the position of stations relative to the ridges is not respected [see *Tison et al.*, 2008].

2004, in close (few meters) proximity to each other. The ice cover was homogeneous, unflooded (positive freeboard) first-year sea ice about 90 cm thick, with a thin snow cover (6–25 cm). The potential scenario of the sea ice cover decay (Figure 1) was discussed extensively elsewhere [*Tison et al.*, 2008]. In short, at the beginning of the observation period, the brine network was unstable in terms of density, as shown by computed brine salinity profiles (Figure 2b). Calculated relative brine volumes ranged from 9% to 33% (Figure 2a) and, therefore, were well above the 5% threshold for increased permeability and connectivity in columnar ice [*Buckley and Trodhal*, 1987; *Golden et al.*, 1998, 2007; *Golden*, 2003]. This suggests that brine inclusions (be it in liquid, gaseous, or particulate form) were largely interconnected throughout the whole sampling period. Large increases of relative brine volumes with time characterized the upper part of the sea ice cover, although important variability may have been related to spatial heterogeneity and potential sampling biases (e.g., partial loss of brine in pockets, channels, or tubes) as sea ice decays [*Tison et al.*, 2008]. Interconnectivity and above-seawater salinities of brines resulted in downward brine migration, especially during stations 29 November to 9 December. Values of $\delta^{18}O$ for bulk sea ice were used to detect changes in the composition of the brines (considering that the signature of the pure ice crystals remained constant with time). On 9 December, decreasing $\delta^{18}O$ values indicated that, as surface brine traveled downward, it was mainly replaced by slush from flooded ridges nearby (lower $\delta^{18}O$ values from snow contribution), whereas internal melting was the main process later on (higher $\delta^{18}O$ values from melting crystals). Increased brine volumes in the upper 50 cm after 9 December also reflected internal melting. Following internal melt, brine salinity dropped below the seawater value in the second half of the observation period (station 14 December onward), which resulted in stratification of the brine network. Under such circumstances, solute exchange is mainly controlled by molecular diffusion processes driven by concentration gradients. Textural observations indicated that superimposed ice formation started in the second half of the period, as melting surface snow infiltrated and refroze at the top of the saltier granular frazil ice. The initial mean ice thickness was 90 ± 0.5 cm. Statistical estimates of the evolution of the ice cover during the observation period corroborate model predictions of a moderate bottom melting (5–10 cm) from ocean heat flux [*Tison et al.*, 2008; *McPhee*, 2008].

3. Materials and Methods

[5] Ice cores were immediately wrapped into PE bags on retrieval and stored on the sampling site in an insulated box filled with individual cooling bags, precooled at −30°C, to limit brine drainage from samples as much as possible. Cores were transported back to the ship as soon as possible and stored at −35°C until further analysis. Holes were drilled into the ice cover at 20 and 60 cm depth (80 cm also on 29 November) to allow gravity-driven brine collection known as the sackhole brine sampling technique [*Thomas and Papadimitriou*, 2003]. Brine and under ice seawater (interface, 1 m, and 30 m deep) were then pumped up using a portable peristaltic pump (Cole-Palmer, Masterflex E/P) and tubing. The preparation and analysis of DMS and DMSP samples from ice is extensively described elsewhere (J. Stefels, The analysis of dimethylsulfide and dimethylsulphoniopropionate in sea ice: dry-crushing and melting using stable isotope additions, submitted to *Marine Chemistry*, 2010). In short, 5 × 3 × 1 cm ice samples were introduced, together with two stainless steel balls, into a stainless steel vessel fitted with two in/out valves. The vessel was kept at −25°C at all times by means of cooling bags, apart from the brief period during which crushing occurred. The vessel was tightly bolted to a custom-made shaker and subjected to fast up-and-down movements. As a result, the ice sample was

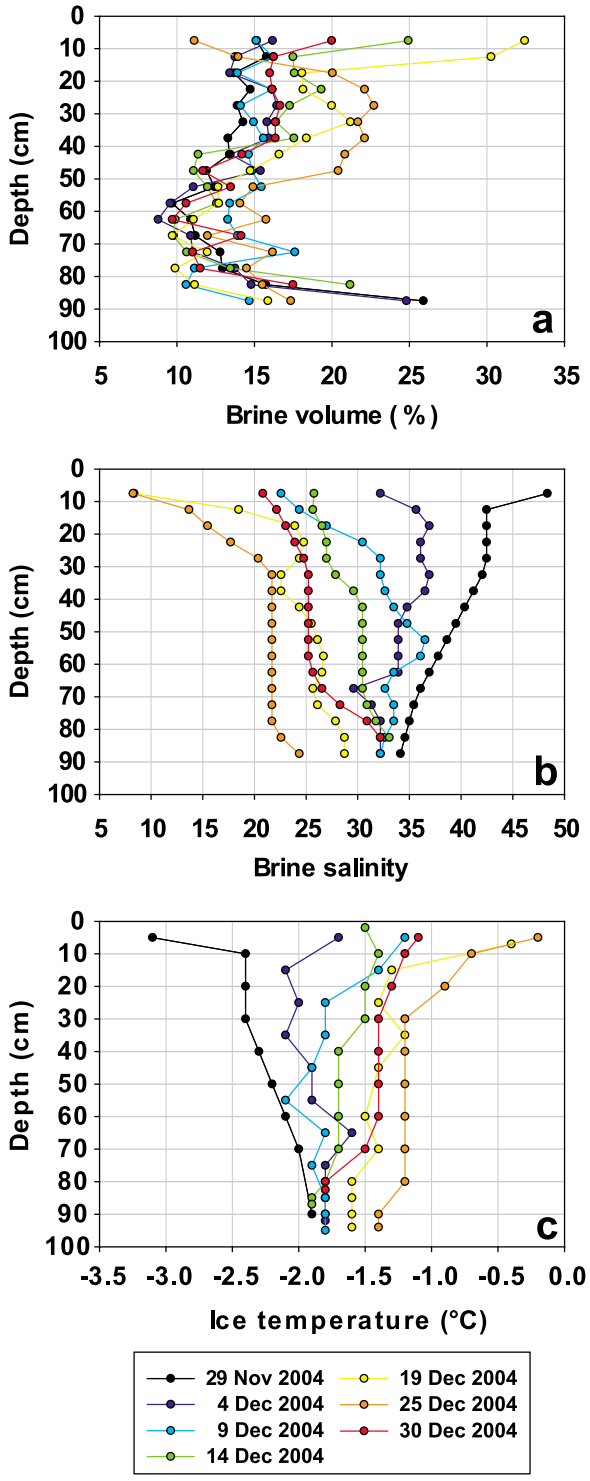

Figure 2. Profiles of computed brine volume and brine salinity in the ice [after *Tison et al.*, 2008].

reduced to a very fine powder. The crushing vessel was then hooked to the inlet line of a proton-transfer-reaction mass spectrometer (PTRMS, Ionicon Analytik, Innsbruck), and the DMS was flushed from the sample with high-purity synthetic air. The principles of proton-transfer-reaction mass spectrometry were described extensively elsewhere [*Lindinger et al.*, 1998; *de Gouw et al.*, 2003; *deGouw and Warneke*, 2007]. Instrument settings for DMS analysis in discrete samples is given in the work of *Stefels et al.* [2009]. After analysis, the ice powder was weighed and a subsample melted in the presence of excess NaOH, to convert total DMSP into DMS after 24 h. The resulting DMS was bubbled from the solution and directly analyzed by PTRMS. Brine and water samples were treated in the liquid state, following the same procedure: first DMS was analyzed and then base was added to convert DMSP into DMS. In those samples in which the solid fraction was analyzed as well, a subsample was filtered gravimetrically over a Whatman GF/F filter and the filtrate was analyzed in two steps as explained earlier in this section. Direct analysis of DMS by PTRMS resulted in an exponentially decaying peak. Total amounts were calculated by integration of peak areas. Calibration curves were prepared from DMS standards (Sigma-Aldrich) in seawater and proved to be linear over more than three orders of magnitude, with typical correlation coefficients larger than 0.999, and a detection limit of 10 pmol DMS [*Stefels et al.*, 2009]. DMS and DMSP concentrations in ice (expressed in n*M*) should be read as nanomoles per kilogram of ice. Discrete chlorophyll *a* measurements were performed at six different depths on a dedicated ice core: two at the top, two in the interior ice, and two at the bottom. Five cm ice core slices (14 cm diam) were collected and melted in a known volume of filtered seawater (1:4 volume ratio) at 4°C, in the dark. The melted samples were then gently filtered onto Whatman GF/F filters using Gelman filtration devices. The filters were stored in cryovials at −80°C for chlorophyll *a* measurements back in the home laboratory. They were extracted in acetone (90% vol/vol) in the dark at 4°C for 24 h, and quantified with a Kontron SFM 25 fluorometer (Kontron Instruments, Neufahrn, Germany) at excitation and emission wavelengths of 430 and 672 nm, respectively, according to the work of *Yentsch and Menzel* [1963]. Ice core sections sampled for the determination of abundance and biomass of microorganisms were melted in the same manner as for the chlorophyll *a* analysis described earlier and analyzed as fully described in the work of *Dumont et al.* [2009]. To compare DMS(P) concentrations in sackholes with those in ice, potential sackhole concentrations were calculated from bulk-ice DMS(P) concentrations, assuming that sackhole brines are a homogeneous mixture of brine material seeping out from the entire ice column above. First, at each depth, DMS(P) concentrations in ice were converted to brine concentrations by multiplying by the density value of 0.91 for first-year sea ice [*Timco and Frederking*, 1996] and dividing by the corresponding relative brine volume as calculated from observed bulk ice salinity and temperature [*Cox and Weeks*, 1983; *Lepparänta and Manninen*, 1988; *Eicken*, 2003]. Subsequently, potential DMS(P) concentrations in sackholes were calculated by averaging reconstructed brine concentrations above the sackhole depth.

4. Results

[6] The highest chlorophyll *a* values (up to 30 μg L^{-1}) were observed in the lowest 10 cm of the ice cover (Figure 3a). Although bottom melting occurred, no systematic change in chlorophyll *a* was found in these layers. A secondary maximum (1–2 μg L^{-1}) occurred in the surface layer on 9

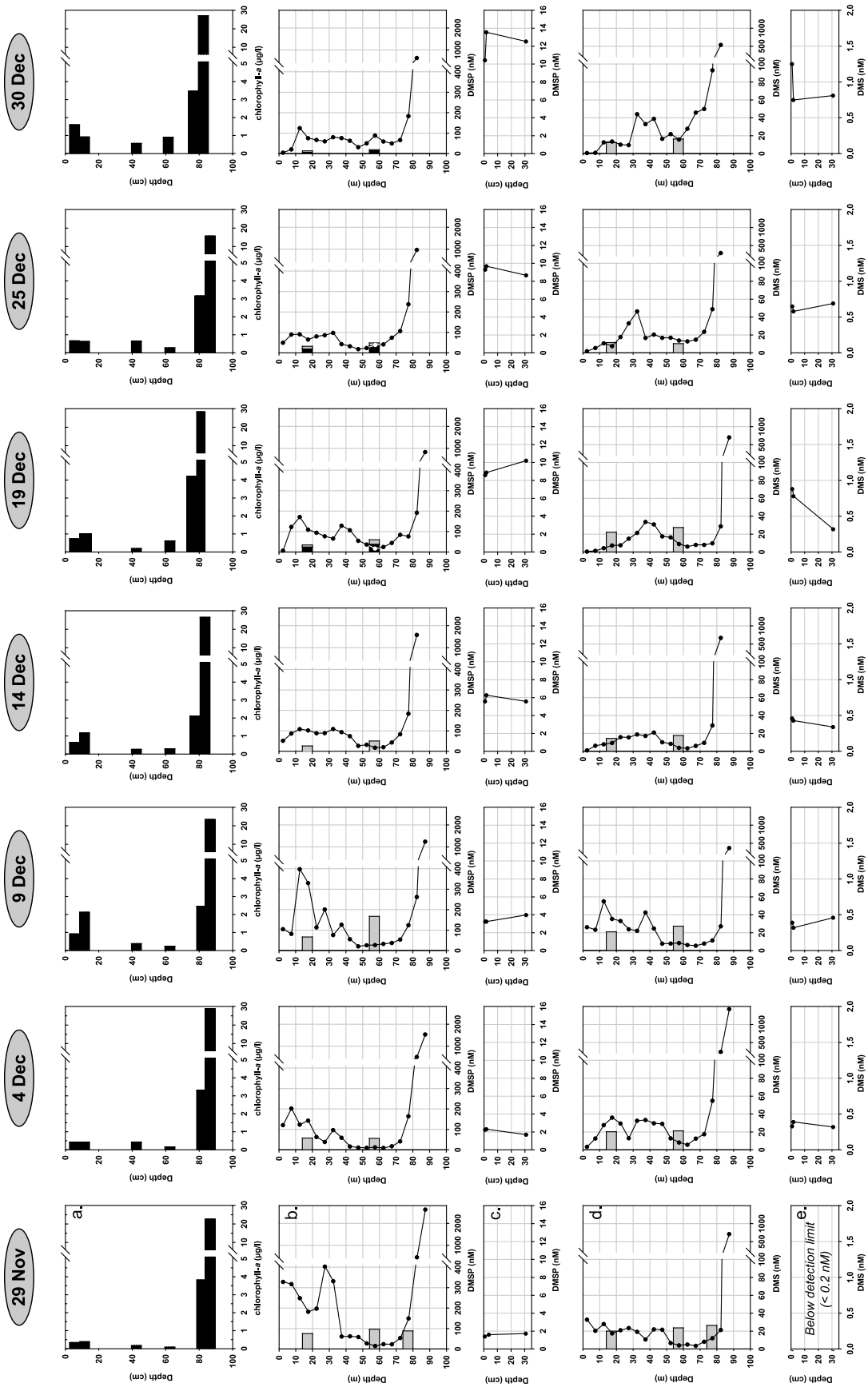
29 Nov
4 Dec
9 Dec
14 Dec
19 Dec
25 Dec
30 Dec
a.
b.
c.
d.
e.
Depth (cm)
chlorophyll-a (µg/l)
Depth (m)
DMSP (nM)
DMS (nM)
Below detection limit
(< 0.2 nM)

Figure 3

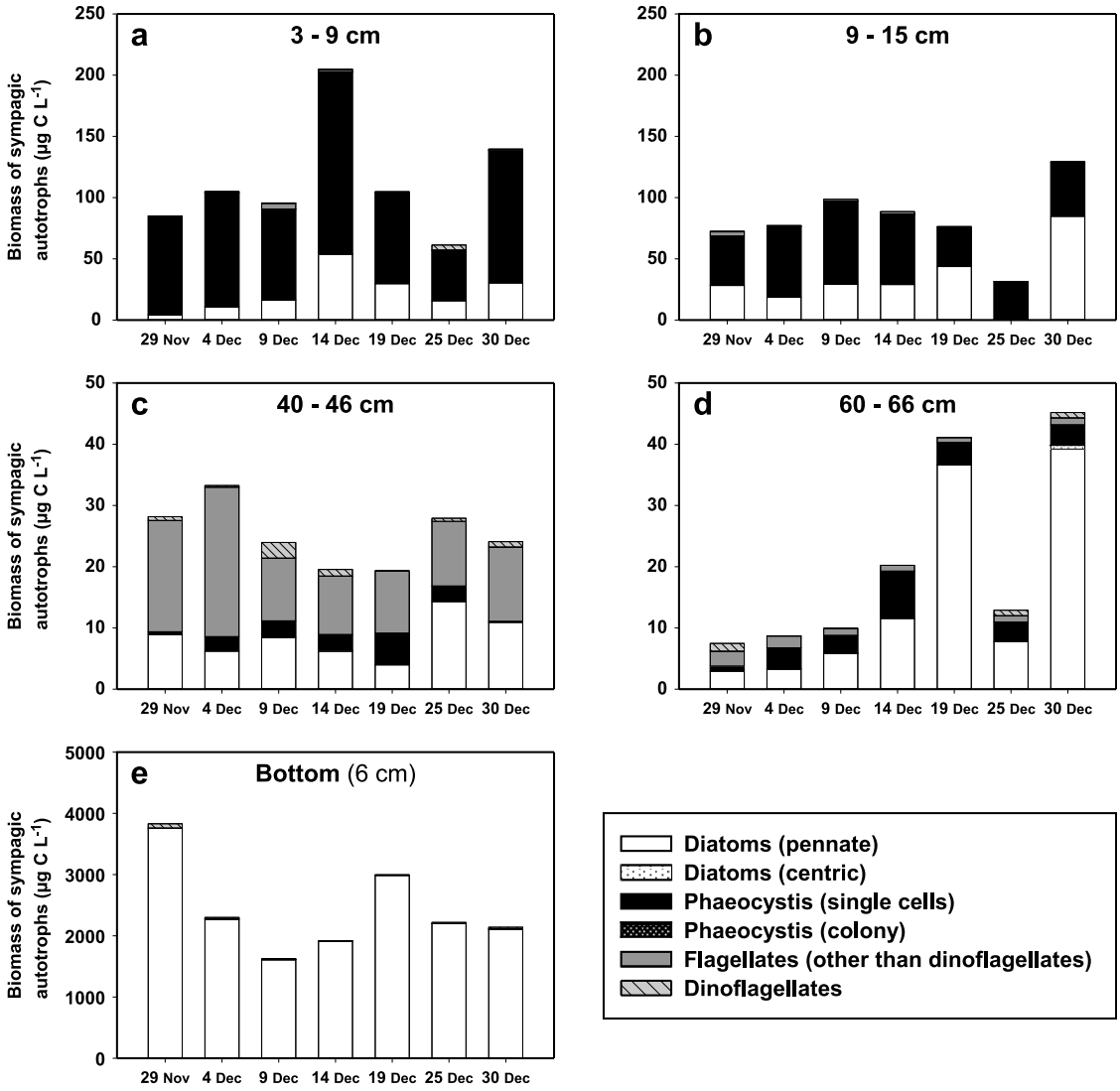

Figure 4. Autotrophic biomass composition observed at five different depths in the ice. Note the difference in vertical scale for the top layers (3–9 and 9–15 cm), the interior layers (40–46 and 60–66 cm), and the bottom (partly from *Dumont* [2009]).

December. Otherwise, chlorophyll *a* remained mostly below 1 μg L^{-1} throughout the upper 70 cm of the sea ice cover for the whole period, though we might have missed some features due to discontinuous sampling. Biomass of sea ice algae was determined at five different depths in the ice corresponding to those where chlorophyll *a* was determined (Figure 4). Autotrophic biomass ranged from 32 to 205 μg CL^{-1} in the top 15 cm (Figures 4a and 4b). Throughout the whole observation period, assemblages in this layer were mainly dominated by *Phaeocystis* sp., which accounted for 34%–95% of the total autotrophic biomass. Pennate diatoms also contributed significantly to the upper ice assemblages with a biomass ranging from 0% to 66% of the total autotrophic biomass. The contribution of the other identified taxa (centric diatoms, dinoflagellates, and other flagellates) to the autotrophic biomass amounted to generally less than 2%. The highest autotrophic biomass levels (from 1622 to 3830 μg C L^{-1}) were observed in the bottom 6 cm of the ice, where pennate diatoms systematically dominated the assemblage, accounting for 98%–100% of the autotrophic biomass (Figure 4e). The lowest levels of autotrophic biomass (from 7 to 45 μg C L^{-1}) were observed in interior ice (Figures 4c and 4d). The upper interior layer (Figure 4c) was most of the time dominated by flagellates (other than dinoflagellates), which

Figure 3. Evolution of (a) ice chlorophyll *a*, (b) ice DMSP (black dots) and brine DMSP (horizontal shaded bars show $DMSP_t$ concentration at the sackholes depth, and $DMSP_p$ proportion is shown as black area on the horizontal bars for the last three stations), (c) underlying seawater DMSP, (d) ice DMS (black dots) and brine DMS (horizontal shaded bars), and (e) underlying seawater DMS at the ISPOL clean site. DMS and DMSP concentrations in ice expressed in n*M* should be read in nanomoles per kilogram of ice.

represented 38%–73% of the total autotrophic biomass at that depth in the ice. The lower interior ice level (Figure 4d) was characterized by a relatively well mixed assemblage at the beginning of the observation period (pennate diatoms, 39%; flagellates, 33%; dinoflagellates, 17%; and *Phaeocystis* sp., 11%) and became largely dominated by pennate diatoms (from 59% to 89% of the total autotrophic biomass) from 9 December onward. A more detailed analysis can be found in the work of *Dumont et al.* [2009]. The evolution in time of total DMSP and DMS in ice profiles is given in Figures 3b and 3d, respectively. DMSP values in the ice spanned the whole range between a few n*M* and about 2600 n*M*, with maximum values localized within the levels of maximum chlorophyll *a*. Two secondary DMSP maxima (300–400 n*M*) were initially present in the upper half of the sea ice cover (one subsurface and one at about 30 cm depth). The subsurface one was associated with relatively low chlorophyll *a* levels. These maxima rapidly diminished (station 4 December) and stabilized at a mean value around 100 n*M* for the rest of the period, with the noticeable exception of station 9 December, which displayed a broad maximum (up to 400 n*M*) between 10 and 40 cm depth, with a corresponding increase of chlorophyll *a* visible in the top 15 cm. The bimodal structure of the upper DMSP maxima, however, remained present throughout the observation period. The interior ice (45–75 cm) showed typical DMSP values of a few tens of n*M*, with no obvious trend with time. In contrast to chlorophyll *a* levels, DMSP concentrations in the lowest 15 cm on average reduced in time. DMS values in the ice (Figure 3d), ranged from negligible (upper layers at the end of the period) to values as high as 1500 n*M* in the bottom layers where both DMSP and chlorophyll *a* levels were highest. As for DMSP, the main changes of DMS concentrations occurred in the upper half of the profile. Two events can be distinguished: Initially at about 20 n*M*, DMS increased up to 60 n*M*, somewhat mimicking the double maximum in DMSP at stations 4 and 9 December. From station 14 December onward, DMS concentrations dropped to negligible values near the surface and a linear gradient established toward a maximum of 45 n*M* DMS at about 40 cm depth. The interior ice and bottom layers showed less variability in DMS with time, apart from the last two stations, where concentration levels tended to increase within the interior ice. DMSP values in brine from sackholes ranged between 20 and 167 n*M* (horizontal bars in Figure 3b). Brine DMSP concentrations decreased with time, with most of the changes occurring in the first half of the observation period, in parallel to that observed in the ice from the upper part of the sea ice cover. From 9 December onward, concentrations in samples from 60 cm depth were consistently higher than those from 20 cm depth. Particulate DMSP concentrations in brine are only available for the second half of the observation period. They were always higher than that for dissolved DMSP. DMS concentrations in brines from sackholes (horizontal bars on graphs of Figure 3d) fluctuated between 10 and 30 n*M* and showed less of a reduction in time than DMSP concentrations. At all stations, brine DMS values from the two sampled depths were similar.

[7] DMSP and DMS concentrations in the underlying water (Figures 3c and 3e, respectively) increased steadily with time at all three measured depths. Both increased about one order of magnitude: DMSP increased from about 1.5 to 14 n*M*, and DMS (from <0.2 to 1 n*M*) remained in the subnanomolar range, with the exception of one sample at the ice-water interface during the final station. Profiles of DMS to DMSP ratios in ice (Figure 5a) systematically showed minimum values in the top 20 cm (mean 0.11, range 0.01–0.29), whereas the bottom 5 cm always displayed higher values (mean 0.56, range 0.27–0.93). The interior ice layer above 60 cm depth was the most dynamic, with a maximum at all stations between 40 and 55 cm. Starting from a maximum value of 0.37 on 29 November, the DMS-to-DMSP ratio reached its maximum value at 50 cm depth on station 4 December (2.75). The ratio rapidly diminished on 9 December with a maximum value of 0.44 and then increased again toward the end of the observation period (0.89 on 25 December). At the last station, a remarkable increase of the ratio in the bottom 20 cm was observed. DMS-to-DMSP ratios in the underlying water column (Figure 5b) reduced in time from approximately 0.17 to 0.06 (mean of the 1 and 30 m depth samples). Profiles of DMSP-to-chlorophyll *a* ratios (Figure 5c) showed relatively high and variable values (mean, 169 nmol μg^{-1}; range, 13–946 nmol μg^{-1}; and standard deviation, 187 nmol μg^{-1}). Owing to the discrete nature of the chlorophyll *a* data and the fact that these data were obtained from a different core than DMSP data, results should be treated with care. Again two phases could be distinguished: During the first two stations, peak values were observed in the subsurface samples, whereas this feature disappeared completely from 9 December onward. The maxima observed in interior ice on 14 and 19 December resulted from relatively low chlorophyll *a* levels, not from high DMSP concentrations, and it is difficult to judge whether this is a firm feature. The relationship between DMSP and chlorophyll *a* concentrations shows a positive linear trend ($R^2 = 0.706$; $P < 0.001$; Figure 6a). There is also a fairly good relationship between DMS and chlorophyll *a* concentrations ($R^2 = 0.818$; $P < 0.001$) (Figure 6b). However, these positive correlations are mainly shaped by the extremely high values of all parameters in the bottom ice layers. When these relationships at chlorophyll *a* levels lower than 5 $\mu g\ L^{-1}$(top and internal layers) were investigated, no significant trend could be observed.

5. Discussion

5.1. DMSP and DMS Ranges

[8] The observed range (5–2627 n*M*) and mean value (171 n*M*) of DMSP at the ISPOL clean site are similar to what was previously reported in the literature for spring-summer pack ice (Table 1). DMSP maximum values reported in this study are, however, the highest ever observed in Antarctic sea ice, except for the extremely high values measured in a particular case of thick rafted sea ice (concentration up to 13,525 n*M* of DMSP measured in an interior slush ice layer) [*Trevena and Jones*, 2006]. DMS mean and maximum values were significantly higher than the values previously reported by *Delille et al.* [2007] and *Trevena and Jones* [2006]. Values of under-ice water DMS (range, <0.2–1.2 n*M*; mean, 0.5 n*M*) and DMSP (range, 2–14 n*M*; average, 6 n*M*) were consistent with values previously observed in under-ice seawater [*Gibson et al.*, 1990; *Kirst et al.*, 1991; *Trevena and Jones*, 2006].

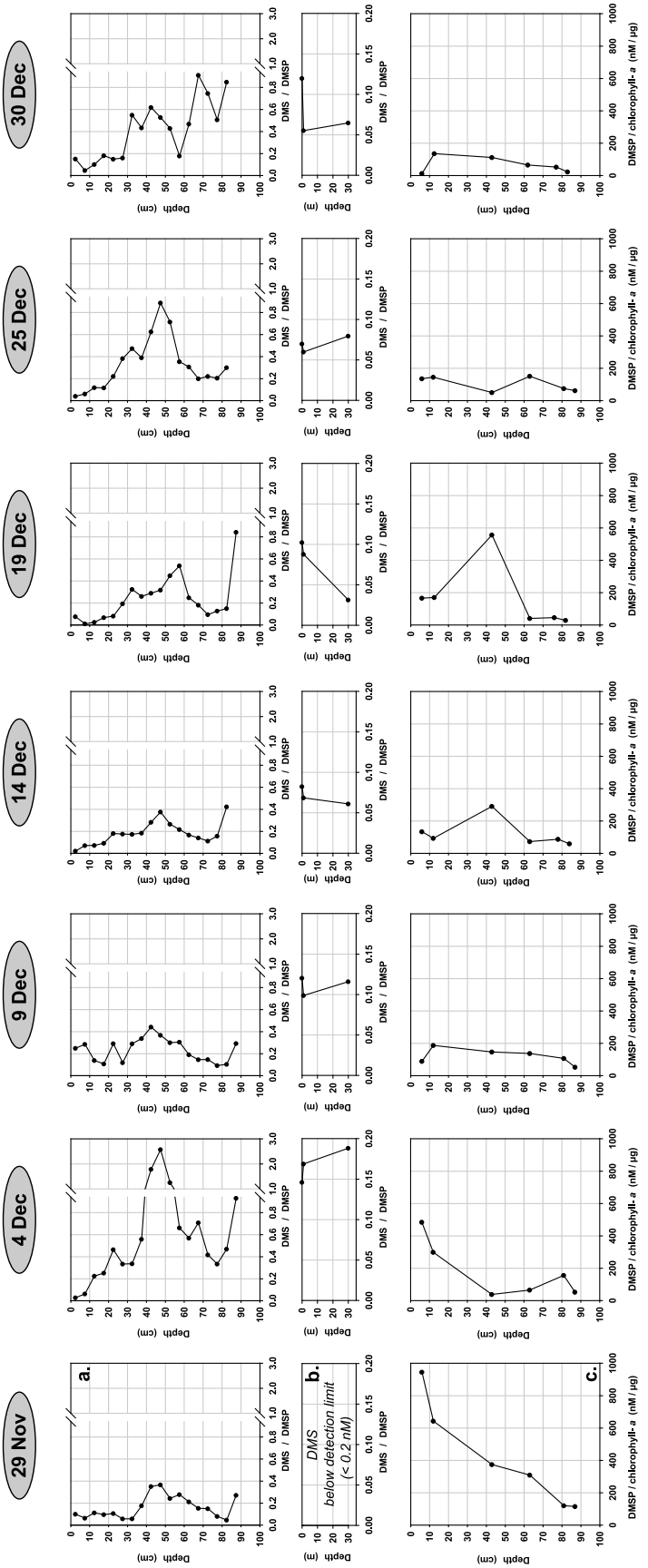

Figure 5. Evolution of (a) DMS-to-DMSP ratio in the ice, (b) DMS-to-DMSP ratio in the underlying seawater, and (c) DMSP-to-chlorophyll *a* in the ice at the ISPOL clean site.

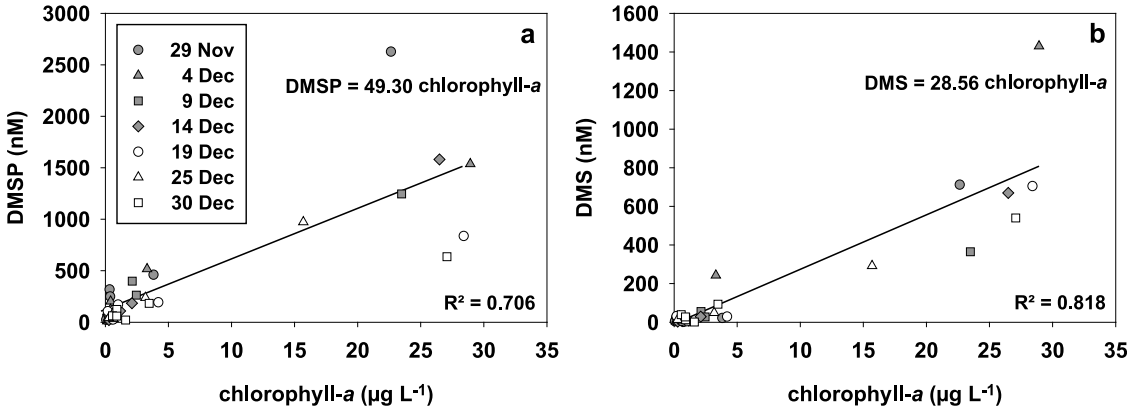

Figure 6. Relationships between chlorophyll *a* and (a) DMSP and (b) DMS at six different depths in the ice.

5.2. DMSP and DMS Dynamics in the Ice

[9] In this section, we discuss both the initial status and the temporal evolution of the DMSP and DMS concentrations within the sea ice cover. Because of the strong contrasts in microbial communities and temporal variability of the thermohaline regime (higher sensitivity in the surface layers as compared to the bottom part), we treat bottom communities and surface and interior communities separately.

5.2.1. Initial Concentration and Temporal Evolution of the DMSP and DMS Profiles in the Bottom Layer

[10] Available chlorophyll *a* (Figure 3a) and autotrophic biomass data (Figure 4) indicate that active primary producers were mainly located in the bottom community. The fairly good linear positive relationship between chlorophyll *a* concentration and DMSP levels (Figure 6a) suggests close links between algal biomass and DMSP concentrations. As previously emphasized by *Levasseur et al.* [1994], it is interesting to note that, although they are known as less efficient DMSP producers compared to *Phaeocystis* sp. or dinoflagellates [*Stefels et al.*, 2007], diatoms are in this case the key drivers of the overall DMSP stock within our sea ice cover at the ISPOL clean site. Note, however, that a different conclusion might have been reached in other areas of the ISPOL floe where flooding of the surface resulted in the development of high biomasses in surface communities of *Phaeocystis* sp. (not shown). There is also a good linear relationship between chlorophyll *a* and DMS. This increase of the DMS content with chlorophyll *a*, especially in the bottom 5 cm where chlorophyll *a* content is above 15 μg L^{-1} (Figure 6b), suggests that, as DMSP production is increased, the various processes leading to the cleavage of DMSP into DMS are also increased (see the work of *Stefels et al.* [2007] for a thorough review of all potential processes). As DMS concentration increases in the bottom layer, so does the DMS-to-DMSP ratio (ranging from 27% to 93%, Figure 5a). Such an increase of the DMS-to-DMSP ratio cannot be attributed to a community shift of autotrophic species because the bottom assemblage remained at all times largely dominated by pennate diatoms (Figure 4). However, protozoa biomass showed a drastic change on 30 December, compared to the previous stations. The biomass of heterotrophic dinoflagellates suddenly peaked at over 550 μg C L^{-1} in the bottom ice of station 30 December, whereas their biomass was below 15 μg C L^{-1} for station 29 November to 25 December [*Dumont*, 2009]. This heterotrophic dinoflagellate population may have exerted an increased grazing pressure on autotrophic DMSP producers of the bottom ice. Grazing by heterotrophic dinoflagellates already proved to be a determining process in the generation of the dissolved pool of DMS and dissolved DMSP (DMSP$_d$) [*Archer et al.*, 2001].

5.2.2. Initial Conditions in the Upper Layers

5.2.2.1. Subsurface DMSP Maximum

[11] The existence of an initial secondary maximum (300–400 n*M* DMSP) at about 30 cm depth could be attributed to the ice formation process. Such a process would have resulted in the accumulation of suspended particulate matter at the ice-water interface, and with it particulate DMSP, due to physicochemical processes and its subsequent entrapment in the ice during freezing. Alternatively, the observed DMSP concentration may have originated from a past active autumnal subsurface community. Control measurements of a DMSP profile performed several months later on a twin core (taken at a maximum distance of a few tens of centimeters) in the home laboratory also revealed the presence of a subsurface DMSP maximum at 30 cm on 29 November (not shown), showing this was a general initial feature of the first-year sea ice at the ISPOL clean site. Measurement of continuous gas composition (O_2, N_2) at a 5 cm resolution on the same core revealed oxygen supersaturation and increased O_2/N_2 ratio between 20 and 40 cm depth, witnessing past production of photosynthetic O_2 by an interior algal community (not shown). Even though chlorophyll *a* data are not available at the depth where DMSP peaked, the very low chlorophyll *a* levels (<0.5 μg L^{-1}) available 15 cm above and 10 cm below the occurrence of the 30 cm DMSP maximum (Figure 3b) suggest that the community was not active anymore at the time of sampling. Progressive disappearance of the 30 cm depth oxygen supersaturation (F. Brabant, unpublished data, 2008) at the next stations, as increased permeability and brine instability drainage developed (see previous sections), is also in favor of an algal community that was either previously active or still living in the ice but in a bad physiological state. The observed 30 cm depth DMSP maximum would therefore be, at least partially, the result of past primary production, although passive scavenging or attachment to the ice platelets of the

skeletal layer during ice growth probably contributed to the initial algal entrapment in autumn. Another indication that we are looking at "old" DMSP is the fact that its concentration quickly decreased between 29 November and 4 December as observed for the oxygen supersaturation. *Trevena et al.* [2003] also attributed the occurrence of a high DMSP peak in interior ice to remains of an algal community. The high DMSP -to-chlorophyll *a* ratio these authors observed was explained by assuming that the degradation of chlorophyll *a* had been faster than that of DMSP.

5.2.2.2. Elevated Surface DMSP-to-Chlorophyll *a* Ratios

[12] The ratios of DMSP to chlorophyll *a* observed in this study (mean, 169 nmol μg^{-1}; range, 13–946 nmol μg^{-1}; and SD, 187 nmol μg^{-1}) compare well with the values previously observed in thick Antarctic fast ice (mean, 243 nmol μg^{-1}; range, 1–3200 nmol μg^{-1}; and SD, 440 nmol μg^{-1}) by *Trevena et al.* [2003]. This is particularly high compared to the mean ratio of 52 ± 37 observed in open waters with Haptophytes [*Stefels et al.*, 2007] among them *Phaeocystis antarctica*, well known for its high DMSP content and its ability to form communities in sea ice. Both environmentally dependent physiological processes within algal cells and community species composition affect the DMSP-to-chlorophyll *a* ratio. It was shown that increasing light intensity [*Stefels et al.*, 2007, and references therein] and increasing salinity [*Stefels*, 2000] of the medium both induce higher DMSP-to-C ratios (and indirectly DMSP-to-chlorophyll *a* ratios) in *Phaeocystis* cells. The initial profile of 29 November showing a steady increase of the DMSP-to-chlorophyll *a* ratio toward the surface may illustrate the adaptation of autotrophic organisms in the ice in response to a gradient in light intensity and/or brine salinity both increasing toward the surface. Alternatively, this profile could reflect the strong contrast in the autotrophic community between the bottom layer dominated by pennate diatoms (Figure 4e) and the surface layers dominated by *Phaeocystis* sp., with diatoms being known for lower DMSP-to-chlorophyll *a* ratios [*Stefels et al.*, 2007]. We find further arguments to dissociate these factors in section 5.2.3.2, which discusses the time evolution of the profiles.

5.2.3. Temporal Evolution of the Upper Layers

5.2.3.1. Changes in DMSP and DMS Profiles

[13] As stated above, most of the DMSP concentration changes occurred in the upper part of the ice cover during the first half of the period under a regime of active brine drainage. The specific situation of station 9 December, where concentrations increased drastically in the upper 30 cm, was probably linked with localized surface infiltration of nutrient- and microorganism-rich slush that likely temporarily boosted the primary production within the brine network [*Tison et al.*, 2008]. Increased DMSP levels (about 400 n*M*) were indeed paralleled by increases in algal standing stock (2 $\mu g\ L^{-1}$ chlorophyll *a*). DMSP concentration profiles were less subject to changes during the second half of the period, when the brine network became stratified and transport became limited to settling of particles due to gravity and diffusion along concentration gradients for dissolved elements [*Tison et al.*, 2008]. Differences in DMS profiles between the first and second half of the observation period in the upper part of the sea ice cover also coincided with the change in brine regime. A linear DMS gradient, established between negligible concentration at the surface and a stable 40 n*M* maximum at about 40 cm depth, replaced the initial bimodal structure of the profile as the brine system switched from downward drainage to stratification (14 December onward). Several mechanisms can explain this sudden decrease of DMS in the upper 40 cm. As indicated by *Tison et al.* [2008], the large increase in relative brine volume between 14 and 30 December may have caused partial loss of brines and gaseous inclusions upon ice core retrieval, even though caution was taken to cool down the cores just after extraction. However, the fact that a gradient was still clearly observed at all stations after 14 December (as opposed to no trend or total loss) does not support a dominant impact of such a sampling bias. Another potential mechanism for the observed DMS gradient is photo-oxidative conversion to DMSO within the surface layers. However, we do not have indications for such a mechanism. Ongoing DMSO measurements show very stable profiles in the upper half of the sea ice cover from 14 December onward, with even a subsequent decrease in the top 30 cm for the last two stations (F. Brabant, unpublished data, 2008). Alternatively, increasing permeability could favor DMS transfer to the atmosphere and therefore establish the observed gradient, provided a source existed in the intermediate layers (see section 5.2.3.3). As discussed by *Tison et al.* [2008], discontinuous superimposed ice was only observed to form during the last two stations and therefore would only have hampered DMS fluxes to the atmosphere at the end of the observation period. Direct CO_2 flux measurements at the ice surface showed that the influx of CO_2 was indeed hampered during the last two sampling dates and could be reestablished by removing the superimposed ice layer (B. Delille, personal communication, 2008). The moderate increase in DMS observed for the last two stations in the lower interior ice (below 60 cm) was probably linked to diffusion processes from the steady bottom maximum upward within the stratified brine medium as the decaying season proceeded and as the DMS production in the bottom community increased.

5.2.3.2. Decrease of the DMSP-to-Chlorophyll *a* Ratio in the Surface Layers

[14] Figure 5c clearly shows a strong decrease of the DMSP-to-chlorophyll *a* ratio in the surface layers during the first half of the observation period. As shown in Figure 7, there is a fairly good relationship between computed brine salinity and DMSP-to-chlorophyll *a* ratio in the upper 12.5 cm for all stations. This simultaneous decrease of DMSP-to-chlorophyll *a* ratio and brine salinity as a consequence of the progressive dilution of the sea ice brine with meltwater during sea ice decay might be interpreted as a physiological adaptation but might also reveal a general community shift with time. In the latter case, species characterized by a lower DMSP-to-chlorophyll *a* ratio (e.g., diatoms at the expense of *Phaeocystis* sp.) would have progressively become dominant in the community. The evolution of the autotrophic biomass with time in the upper layer (Figures 4a and 4b), however, supports the hypothesis that the change of DMSP-to-chlorophyll *a* ratio was rather driven by the brine salinity drop. No drastic change in the contribution of the different species to the autotrophic biomass (almost systematically dominated by *Phaeocystis* sp.) was observed from 29 November to 9 December when most of the change occurred in the ratio of DMSP to chlorophyll *a*.

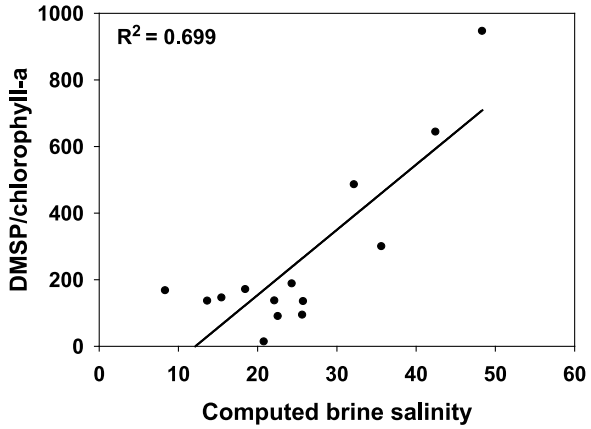

Figure 7. Values of DMSP-to-chlorophyll *a* ratio against computed brine salinity in the upper 12.5 cm of the sea ice cover.

5.2.3.3. DMSP-to-DMS Conversion

[15] To investigate the conversion dynamics of DMSP into DMS in the ice, we consider hereafter the evolution of the DMS-to-DMSP ratio (Figure 5a). A few common features characterize all stations, independent of time. First, the DMSP originally linked to algal cells fixed to the walls of brine channels and brine pockets was released into the brine medium (see section 5.3) throughout the observation period as a result of the progressive rise in temperature and consequential internal ice melting. Second, all stations showed a layer of minimum brine volume located between 55 and 70 cm depth (Figure 2a) potentially acting as a local constriction of the sea ice brine network, slowing down the downward movement of solutes and particulate matter. Indeed, even after the interconnectivity of the brine network has been reestablished above the 5% brine volume threshold, permeability still increases with increasing brine volume [e.g., *Golden et al.*, 2007]. Finally, the DMS-to-DMSP ratio (Figure 5a) indicated that conversion of DMSP to DMS occurred above the area of brine network constriction. The active brine drainage that characterized the first phase of the observation period (stations 29 November and 4 December) induced an effective downward transfer to the level of minimum brine volume of both DMS and DMSP available in the brine network, favoring accumulation of material in the layers above the brine network constriction. The local maximum of the DMSP-to-chlorophyll *a* ratio that developed at about 40 cm depth at stations 14 and 19 December (Figure 5c) may indicate that the local accumulation of degrading algal cells indeed occurred, because such an increase cannot be explained by either an increase in light intensity or an increase in brine salinity. Also, there have been no significant changes in the contribution of different species to the autotrophic assemblage (Figure 4c). The slush infiltration event that occurred at station 9 December [*Tison et al.*, 2008] is likely responsible for the more homogenous DMS/DMSP profile observed. The increased transfer of solutes (along with DMS and DMSP in the brine) through the brine network down to the seawater would have made the DMS/DMSP profile more uniform than the profile of the previous station. Note, however, that this could also be the result of spatial variability since station 9 December was located closer to border ridges and therefore more prone to slush infiltration. The second phase of the observation period (from station 14 December onward), however, is characterized by a drastic slowdown in fluid movement and solute transport through the ice cover because of the stratification of the sea ice brine network. This stratification implies that DMSP released from the brine channels or brine pocket walls overhead was transferred more slowly downward by sedimentation through the brine network. DMSP therefore accumulated at a lower rate above the depth of minimum porosity than under the influence of brine drainage. The lower rate of DMSP accumulation would have slowed down the production of DMS and delayed the new buildup of the DMS/DMSP maximum. In addition, the intensity of the DMS/DMSP maximum must have been affected by the rate of DMS loss either through brine drainage (first phase) or diffusion (second phase), especially toward the atmosphere as suggested by DMS profiles. Several factors may explain the conversion of DMSP to DMS in this particular zone. Exudation of DMSP by some algal species in the surrounding environment may have occurred in response to the brine dilution caused by the steady internal ice melting. Such aprocess has already proven to occur with some algal species (*Phaeocystis* sp.) in response to a salinity decrease in the environment [*Stefels and Dijkhuizen*, 1996]. In situ conversion of $DMSP_d$ to DMS may have occurred under the influence of algal or bacterial DMSP lyase, a salinity decrease being additionally favorable to the enzyme activity [*Stefels and Dijkhuizen*, 1996]. Heterotrophic dinoflagellates and ciliates were also observed to increase in this layer, although at lower concentrations than in the bottom layer [*Dumont*, 2009]. They also may have played a role in the production of DMS by grazing on autotrophic DMSP producers like *Phaeocystis* sp. and dinoflagellates [*Archer et al.*, 2001]. Along the same lines, the general increase of the DMS-to-DMSP ratio below 60 cm is very likely attributed to the sudden increase of heterotrophic dinoflagellates, which would be responsible for an increased DMS production by grazing as stated earlier.

5.3. DMSP and DMS Dynamics in the Brine

[16] DMS(P) concentrations from 20 cm depth sackhole brines appeared to be lower than the concentrations measured in bulk ice samples. This finding was unexpected, considering that pure ice crystals are devoid of the two compounds, and brines formed between 9% and 33% of the bulk sea ice volume (Figure 2a). Also DMS(P) concentrations from 60 cm depth sackhole brines, although both relatively and absolutely higher than brines from 20 cm depth, were still lower than expected. One way to visualize that concept is to reconstruct DMSP and DMS concentrations in the brine from observed bulk ice values and relative brine volumes. Results of this exercise are shown in Figures 8a (DMSP) and 8b (DMS). Clearly, both calculated DMSP and DMS concentrations are higher than measured values by a factor of up to 20. As far as DMSP is concerned, this can be explained with a well-known feature that algal cells are mainly fixed to the walls of brine channels and pockets rather than floating freely into the brine medium [*Krembs et al.*, 2002]. Algae biomass percentage attached to brine channel walls evolved from 97% to 57% during the ISPOL experiment (S. Becquevort, personal communication, 2008).

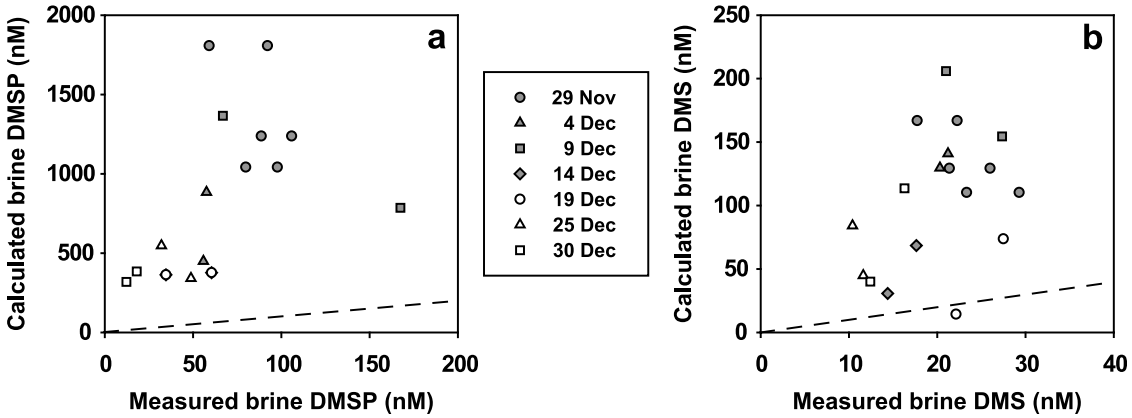

Figure 8. (a) Relationship between measured brine DMSP and calculated brine DMSP and (b) relationship between measured brine DMS and calculated brine DMS. The dashed line represents a one-to-one relationship. Note the difference in vertical and horizontal scales between Figures 8a and 8b.

This can be explained by the increasing release into the brine medium of material fixed to the walls of brine inclusions (including intracellular or particulate $DMSP_p$) by melting. Such a process is confirmed by our observation that the discrepancy between measured and reconstructed brine DMSP values became globally smaller as the sea ice cover decayed. The fact that DMSP concentrations from 20 cm depth sackholes are generally lower than those at 60 cm and further below the bulk ice values, especially at the first two stations, may be attributed to a lower ice temperature toward the surface. Reduced melting at lower temperatures indeed releases a smaller amount of particulate material into the sackhole, because that material still adheres to the brine inclusions walls.

[17] Differences between observed and reconstructed brine DMS values were less expected, because that compound should essentially exist as a solute in the brine medium. The only plausible explanation, which is in accordance with the observed DMS profiles in the ice of the upper layers during the second half of the observation period, is that the in situ production of DMS was so important that it maintained high levels of concentration at all times well above saturation. These were then potentially responsible for substantial losses during sackhole brine collection, either through bubbles degassing or through enhanced diffusion. DMS concentration in brines in equilibrium with the atmospheric DMS concentration values (from 0.2 to 5 nmol m^{-3}), measured by *Zemmelink et al.* [2008] during the same experiment, were calculated. According to *Dacey et al.* [1984], DMS in seawater at −0.8°C (average temperature of the brine within the top 20 cm of the ice from stations 19 to 30 December) has a Henry's constant of 0.676. Considering an average air temperature of −4.8°C during the study period and the atmospheric DMS concentration values measured by *Zemmelink et al.* [2008], DMS partial pressure ranged from 4.4×10^{-12} atm to 1.1×10^{-10} atm. The DMS concentration in seawater in equilibrium with the latter partial pressure range from 6.5×10^{-3} n*M* to 1.6×10^{-1} n*M*, which is two to four orders of magnitude less than the concentration measured in the brines collected at 20 cm depth (from 11 to 22 n*M*). As a result, high concentration gradients were established with the atmosphere leading to substantial losses of DMS, especially for the brine accumulating in the sackholes as compared to those sampled together with the bulk ice. Furthermore, if supersaturation had led to DMS-rich bubble formation in the ice, these would have been detected by the dry extraction technique, while clearly escaping from the collected sackhole brines, strengthening the discrepancy. Again, the latter was likely to be reduced as the warming of the sea ice progressed and as the brine volume increased drastically in the upper layers of the sea ice cover, potentially enhancing exchange of the bulk ice DMS with the atmosphere or with the snow pack above (Figure 8b). A complementary process that would sustain these enhanced exchanges is presented in section 5.4.

5.4. DMSP and DMS Dynamics in the Water

[18] Both DMSP and DMS concentration increased with time in the water underneath the sea ice cover. Concentration levels, however, remained quite low (1%–5%) as compared to the values observed within the bottom ice layers (Figures 3c and 3e). Figure 5b also shows that initially, with the exception of station 29 November, the relative proportion of DMS was higher, possibly reflecting the contribution from brine drainage during the first half of the observation period. Later on, the relative proportion of DMSP in the water increased, probably as a result of the progressive release into the brine medium of DMSP fixed to the brine channel walls. In situ production of DMSP in the water column is indeed less of an option given the very low and constant chlorophyll *a* levels observed during the first half of the observation period (0.03–0.06 μg Chl *a* L^{-1}). Contemporaneous observations of DMS and DMSP concentrations in the leads nearby [*Zemmelink et al.*, 2005] are worth comparing to our data set. Their measurements, performed between 0 and 4 m depth with a decimeter resolution in the upper 30 cm, showed values similar to our water concentrations, below 30 cm depth. However, surface values reached much higher levels of about 45 and 100 n*M* for DMS and DMSP, respectively. These are intermediate between those that were found in sea ice (40 and 100 n*M*) and brine (10–30 and 30–167 n*M*) at the ISPOL clean site. It therefore suggests that a lateral connection was present

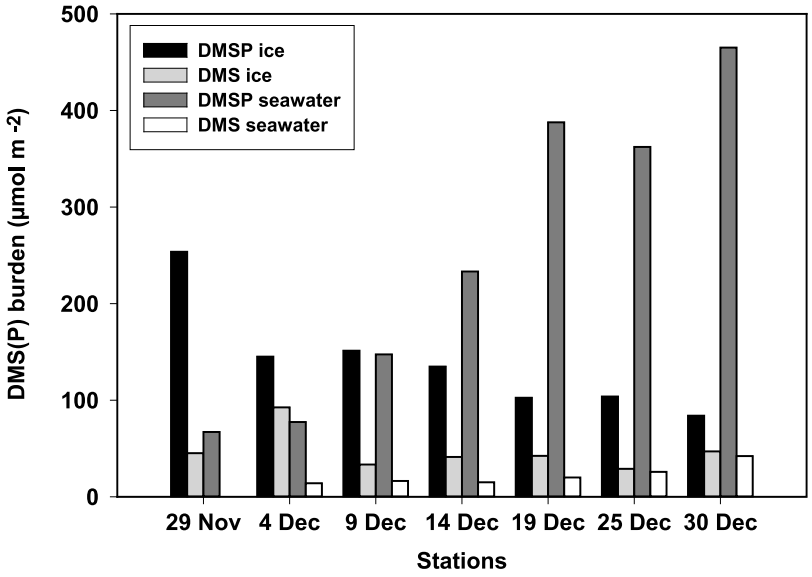

Figure 9. DMSP and DMS burden evolution in the ice and underlying 40 m water column.

between the brine existing within the upper 40 cm honeycomb-like ice layer and the surface waters of the leads. The relatively low salinity of those surface brines (down to 21) favored buoyancy and contribution to the signature of the surface layer of the leads nearby. Together with the patchy biologically enriched flooded surface layers existing in other areas of the ISPOL floe (D. N. Thomas, personal communication, 2006), the honeycomb-like layer that characterizes decaying summer sea ice [*Haas et al.*, 2001; *Ackley et al.*, 2008] was therefore a potentially major contributor to DMS release.

5.5. Impact of Sea Ice on the Regional DMSP and DMS Budget

[19] DMSP and DMS burdens were calculated in the ice and in the water (Figure 9). Clearly, these should only be considered rough estimates. Although the measurements were made on a limited area of the same ice floe, the floe had been drifting for more than 100 km northward during the course of the experiment, thereby partially decoupling the ice cover from underlying sea water at the small scale. However, as far as sea ice is concerned, DMSP burdens decreased regularly throughout the observation period from 254 to 84 μmol m^{-2}. After a peak at 92 μmol m^{-2} on 4 December, DMS burdens stabilized around a mean value of 39 μmol m^{-2} for the rest of the observation period. In the under-ice water column, DMSP and DMS burdens were calculated based on the interface, 1 m, and 30 m measurements and integrated over the mixed layer depth of 40 m [*Absy et al.*, 2008]. DMSP burdens increased steadily from 67 μmol m^{-2} to culminate at 465 μmol m^{-2} on 30 December while DMS burdens slowly increased from 0.4 to 42 μmol m^{-2}. The progressive fall of DMSP burdens in the ice might be seen as a result of DMSP loss to the seawater through brine drainage and in situ conversion to DMS and biological consumption. The occurrence of an ice DMS burden peak on 4 December corresponded with the sharpest decrease of DMSP burden observed between the first two stations, which suggests that a part of the DMSP had likely been converted to DMS in the ice. Stabilization of the ice DMS burden from 9 December onward reflects the fact that a balance was reached between the production of DMS and its removal from the ice through degassing and diffusion to the atmosphere, diffusion to the ice-water interface, photochemical oxidation, and bacterial consumption. The increase of water DMSP burden concurrent with the decrease of ice DMSP burden suggests that sea ice was an important source of DMSP for the water column at that moment of the year. The moderate increase of DMS observed in the underlying seawater is likely to be the result of the balance between the release of DMS and DMSP from sea ice, the conversion of DMSP to DMS in the water column, and the biological or photochemical removal of DMS from the water column [*Slezak et al.*, 2001, 2007].

[20] To assess the impact of sea ice on the regional sulfur budget, total DMSP + DMS fluxes in ice and water were calculated as the difference between the DMS + DMSP burdens of two consecutive sampling days, within ice and water, respectively (Table 2). The constantly negative DMS (P) flux from the ice reflects a continuous loss of DMSP and DMS through different processes of degassing and diffusion of DMS to the atmosphere and downward migration of DMSP and DMS with the draining brines at the beginning of the observation period. The evolution of burdens (Figure 9) clearly shows that most of the flux from the ice was due to DMSP loss. The contrast between the strong fluxes observed for the first two stations, where most of the DMSP and DMS loss rapidly occurred (69% of the total observed loss from the ice occurred between stations 29 November and 9 December), and the rest of the observation period corresponded with the change in brine regime. Rapid loss of DMSP and DMS coincided with the sharpest decrease of salinity observed between the first three stations, reflecting mass transport of solutes through the brine inclusions network under the influence of brine drainage

Table 2. Calculated Total Ice and Water (DMS + DMSP) Flux

	Time Step						
	29 Nov to 4 Dec	4–9 Dec	9–14 Dec	14–19 Dec	19–25 Dec	25–30 Dec	Average Flux
Ice DMS(P) flux[a] (μmol m^{-2} d^{-1})	−12.2	−10.6	−1.7	−6.2	−2.0	−0.4	−5.4
Water DMS(P) flux[a] (μmol m^{-2} d^{-1})	4.8	14.5	16.9	31.9	−3.3	23.8	14.2

[a]A negative value means an outgoing flux.

events [*Tison et al.*, 2008]. This emphasizes the importance of brine drainage in the control of the sea ice DMSP and DMS dynamics during sea ice decay. Integrated fluxes over the whole observation period (average fluxes in Table 2) were of the same order of magnitude as previous regional estimates of 9.4 μmol DMS m^{-2} d^{-1} in the Australian sector of the Southern Ocean [*Curran and Jones*, 2000] and measurement of 11 μmol DMS m^{-2} d^{-1} over the multiyear ice of the ISPOL floe [*Zemmelink et al.*, 2008]. Our estimates, which include the contribution of both DMS and DMSP as well as the loss to the water column, seem low, however, in comparison to the value reported by *Zemmelink et al.* [2008], who solely measured ice-air DMS flux. Given the location of the flux tower on the multiyear ice zone of the ISPOL floe characterized by the presence of algal surface communities known to be highly productive [*Kattner et al.*, 2004], it is reasonable to think that the average flux measured by *Zemmelink et al.* [2008] largely reflected DMS coming from such surface communities. These measured fluxes were also likely widely influenced by DMS emissions from surrounding leads where high DMS levels were observed in the surface microlayer [*Zemmelink et al.*, 2005]. Such contributions of surface communities (not observed at the sampled clean site) and leads were not captured in our estimates. The difference between the calculated average fluxes (DMS + DMSP) from the ice (5.4 μmol DMS(P) m^{-2} d^{-1}) and to the water (14.2 μmol DMS(P) m^{-2} d^{-1}) by a factor of about 3 can have several causes: (1) uncertainty in the reconstruction of water burdens from only three concentration measurements for a 40 m water column; (2) potential decoupling of ice cover from underlying seawater because of ice drift; (3) potential underestimation of DMS and DMSP losses from the ice due to sampling biases, especially in the interface bottom layer; (4) temporal resolution of the flux calculation, implying a potential lack of information on DMS and DMSP production and losses from the ice occurring at rates higher than the 5 day time interval; and (5) the potential in situ algal DMSP production in the water column, which would contribute to the calculated positive flux.

6. Conclusions and Perspectives

[21] For the first time ever, we give a full description and discuss DMS and DMSP high-resolution profiles in sea ice, in a time series perspective. It is shown that the sea ice thermohaline regime plays a major role in controlling the DMS and DMSP dynamics within the sea ice cover, especially in the surface layers and interior of the sea ice cover, owing to the large changes in surface energy balance during spring and summer. This is either directly through the release of DMSP from the brine channel walls and the control of the DMSP and DMS migration within the brine inclusion network or, indirectly, through promoting a physiological response of ice DMSP producers. In this case of the ISPOL clean site, where no flooding of the surface layers with seawater occurred (positive freeboard throughout), DMSP production was dominated by pennate diatoms within the bottom layers, because their much higher biomass overcompensated their known lesser DMSP synthesis efficiency per unit cell.

[22] We produce first estimates of the impact of decaying sea ice on the regional sulfur budget in the Weddell Sea and show that these are of the same order of magnitude as those previously reported in other studies for DMS in Antarctic open waters. Our fluxes are most probably underestimated, given the potentially huge contribution of surface communities that were not present at our study site. However, these estimates already demonstrate that sea ice acts at that moment of the year as an important and continuous source of DMSP and DMS with respect to the ocean and the atmosphere. This study also stresses the lack of available information on physiological adaptation of the ice community toward changing abiotic conditions during sea ice decay and the role DMS(P) metabolism plays in that adaptation. This is a fundamental prerequisite to adequate modeling of sea ice controls on the flux of climatically significant sulfur compounds to the atmosphere. Future work should therefore be dedicated to metabolic studies performed under real conditions where physiological and physicochemical processes can interact. DMSO concentration measurements would also provide essential information to complete the sulfur budget and shed more light on the sulfur cycle dynamics in sea ice. Finally, ongoing studies on algal and microbial determination and relationships to organic matter will certainly provide further clarification of the control processes of DMS, DMSP, and DMSO production and transformation within the sea ice medium.

[23] **Acknowledgments.** The authors greatly thank the Alfred Wegener Institut für Polar- und Meeresforschung for inviting them to join the ISPOL cruise. This research was supported by the Communauté Française de Belgique (SIBClim project, ARC contract 02/07-287). F. Brabant and I. Dumont are supported by a Belgian FRIA grant (Fonds pour la Recherche dans l'Industrie et l'Agriculture, Fonds de la Recherche Scientifique). J. Stefels was financially supported by the Polar Program of the Dutch National Science Foundation (NWO/ALW-NPP project 851.20.022). The authors greatly acknowledge J. W. H. Dacey for helping in data treatment, fruitful discussions, and sample collection in the field.

References

Abram, M., R. Mulvaney, E. W. Wolff, and M. Mudelsee (2007), Ice core records as sea ice proxies: An evaluation from the Weddell Sea region of Antarctica, *J. Geophys. Res.*, *112*, D15101, doi:10.1029/2006JD008139.

Absy, J. M., M. Schröder, R. Muench, and H. H. Hellmer (2008), Early summer thermohaline characteristics and mixing in the western Weddell Sea, *Deep Sea Res., Part II*, *55*, 1117–1131, doi:10.1016/j.dsr2.2007.12.023.

Ackley, S. F., M. J. Lewis, C. H. Fritsen, and H. Xie (2008), Internal melting in Antarctic sea ice: Development of "gap layers", *Geophys. Res. Lett.*, *35*, L11503, doi:10.1029/2008GL033644.

Archer, S. D., C. E. Stelfox-Widdicombe, P. H. Burkill, and G. Malin (2001), A dilution approach to quantify the production of dissolved dimethylsulphoniopropionate and dimethyl sulphide due to microzooplankton herbivory, *Aquat. Microb. Ecol.*, *23*(2), 131–145, doi:10.3354/ame023131.

Buckley, R. G., and H. J. Trodhal (1987), Thermally driven changes in the optical properties of sea ice, *Cold Reg. Sci. Technol.*, *14*(2), 201–204, doi:10.1016/0165-232X(87)90036-X.

Charlson, R. J., J. E. Lovelock, M. O. Andreae, and S. G. Warren (1987), Oceanic phytoplankton, atmospheric sulphur, cloud albedo and climate, *Nature*, *326*, 655–661, doi:10.1038/326655a0.

Cox, G. F. N., and W. F. Weeks (1983), Equations for determining the gas and brine volumes in sea-ice samples, *J. Glaciol.*, *29*(102), 306–316.

Curran, M. A. J., and G. B. Jones (2000), Dimethylsulfide in the Southern Ocean: Seasonality and flux, *J. Geophys. Res.*, *105*(D16), 20,451–20,461.

Curran, M. A. J., T. D. van Ommen, V. I. Morgan, K. L. Phillips, and A. S. Palmer (2003), Ice core evidence for Antarctic sea ice decline since the 1950s, *Science*, *302*, 1203–1206.

Dacey, J. W. H., S. G. Wakeham, and B. L. Howes (1984), Henry's law constants for dimethylsulfide in freshwater and seawater, *Geophys. Res. Lett.*, *11*(10), 991–994, doi:10.1029/GL011i010p00991.

de Gouw, J., and C. Warneke (2007), Measurements of volatile organic compounds in the Earth's atmosphere using proton-transfer-reaction mass spectrometry, *Mass Spectrom. Rev.*, *26*, 223–257.

de Gouw, J., C. Warneke, T. Karl, G. Eerdekens, C. van der Veen, and R. Fall (2003), Sensitivity and specificity of atmospheric trace gas detection by proton-transfer-reaction mass spectrometry, *Int. J. Mass Spectrom.*, *223*, 365–382.

Delille, B., B. Jourdain, A. V. Borges, J.-L. Tison, and D. Delille (2007), Biogas (CO_2, O_2, dimethylsulfide) dynamics in spring Antarctic fast ice, *Limnol. Oceanogr.*, *52*(4), 1367–1379.

DiTullio, G. R., D. L. Garrison, and S. Mathot (1998), Dimethylsulfonopropionate in sea ice algae from the Ross Sea polynya, in *Antarctic Sea Ice: Biological Processes, Interaction and Variability*, *Antarct. Res. Ser.*, vol. 73, edited by M. Lizotte and K. Arrigo, pp. 139–146, AGU, Washington, D. C.

Dumont, I. (2009), Interactions between the microbial network and the organic matter in the Southern Ocean: Impacts on the biological carbon pump, Ph.D. thesis, Fac. des Sci., Univ. Libre de Bruxelles, Brussels.

Dumont, I., V. Schoemann, D. Lannuzel, L. Chou, J.-L. Tison, and S. Becquevort (2009), Distribution and characterization of dissolved and particulate organic matter in Antarctic pack ice, *Polar Biol.*, *32*(5), 733–750, doi:10.1007/s00300-008-0577-y.

Eicken, H. (2003), From the microscopic to the macroscopic to the regional scale: Growth, microstructure and properties of sea ice, in *Sea Ice: An Introduction to Its Physics, Biology, Chemistry and Geology*, edited by D. N. Thomas and G. S. Dieckmann, pp. 22–81, Blackwell Sci., Oxford, U. K.

Gambaro, A., I. Moret, R. Piazza, C. Andreoli, E. D. Rin, G. Capodaglio, C. Barbante, and P. Cescon (2004), Temporal evolution of DMS and DMSP in Antarctic Coastal Sea water, *Int. J. Environ. Anal. Chem.*, *84*(6–7), 401–412, doi:10.1080/03067310310001636983.

Gibson, J. A. E., R. C. Garrick, H. R. Burton, and A. R. McTaggart (1990), Dimethylsulfide and the alga *Phaeocystis pouchetii* in Antarctic coastal waters, *Mar. Biol.*, *104*(2), 339–346, doi:10.1007/BF01313276.

Gleitz, M., M. R. van der Loeff, D. N. Thomas, G. S. Dieckmann, and F. J. Millero (1995), Comparison of summer and winter inorganic carbon, oxygen and nutrient concentrations in Antarctic sea ice brine, *Mar. Chem.*, *51*, 81–91.

Golden, K. M. (2003), Critical behavior of transport in sea ice, *Physica B*, *338*, 274–283, doi:10.1016/j.physb.2003.08.007.

Golden, K. M., S. F. Ackley, and V. I. Lytle (1998), The percolation phase transition in sea ice, *Science*, *282*, 2238–2241.

Golden, K. M., H. Eicken, A. L. Heaton, J. Miner, D. J. Pringle, and J. Zhu (2007), Thermal evolution of permeability and microstructure in sea ice, *Geophys. Res. Lett.*, *34*, L16501, doi:10.1029/2007GL030447.

Haas, C., D. N. Thomas, and J. Bareiss (2001), Surface properties and processes of perennial Antarctic sea ice in summer, *J. Glaciol.*, *47*(159), 613–625.

Kattner, G., D. N. Thomas, C. Haas, H. Kennedy, and G. S. Dieckmann (2004), Surface ice and gap layers in antarctic sea ice: Highly productive habitats, *Mar. Ecol. Prog. Ser.*, *277*, 1–12, doi:10.3354/meps277001.

Keller, M. D., W. K. Bellows, and R. R. L. Guillard (1989), Dimethyl sulfide production in marine phytoplankton, in *Biogenic Sulfur in the Environment*, edited by E. S. Saltzman and W. J. Cooper, pp. 167–182, Am. Chem. Soc., Washington, D. C.

Kirst, G., C. Thiel, H. Wolff, J. Nothnagel, M. Wanzek, and R. Ulmke (1991), Dimethylsulfoniopropionate (DMSP) in ice algae and its possible biological role, *Mar. Chem.*, *35*, 381–388.

Krembs, C., H. Eicken, K. Junge, and J. W. Deming (2002), High concentrations of exopolymeric substances in Arctic winter sea ice: Implications for the polar ocean carbon cycle and cryoprotection of diatoms, *Deep Sea Res., Part I*, *49*, 2163–2181.

Lee, P. A., S. J. de Mora, and M. Gosselin (2001), Particulate dimethylsulfoxide in Arctic sea-ice algal communities: The cryoprotectant hypothesis revisited, *J. Phycol.*, *37*(4), 488–499, doi:10.1046/j.1529-8817.2001.037004488.x.

Lepparänta, M., and T. Manninen (1988), The brine and gas content of sea ice with attention to low salinities and high temperatures, *Internal Rep. 88-2*, Finn. Inst. of Mar. Res., Helsinki.

Levasseur, M., M. Gosselin, and S. Michaud (1994), A new source of dimethylsulfide (DMS) for the Arctic atmosphere: Ice diatoms, *Mar. Biol.*, *121*(2), 381–387, doi:10.1007/BF00346748.

Lindinger, W., A. Hansel, and A. Jordan (1998), On-line monitoring of volatile organic compounds at pptv levels by means of proton-transfer-reaction mass spectrometry (PTRMS) medical applications, food control and environmental research, *Int. J. Mass Spectrom. Ion Processes*, *173*, 191–241.

McPhee, M. G. (2008), Physics of early summer ice/ocean exchanges in the western Weddell Sea during ISPOL, *Deep Sea Res., Part II*, *55*, 1075–1097, doi:10.1016/j.dsr2.2007.12.022.

Meyerson, E. A., P. A. Mayewski, K. J. Kreutz, L. D. Meeker, S. I. Whitlow, and M. S. Twickler (2002), The polar expression of ENSO and sea-ice variability as recorded in a South Pole ice core, *Ann. Glaciol.*, *35*, 430–436.

Mulvaney, R., E. C. Pasteur, and D. A. Peel (1992), The ratio of MSA to non-sea-salt sulphate in Antarctic Peninsula ice cores, *Tellus, Ser. B*, 295–303.

Pasteur, E. C., R. Mulvaney, D. A. Peel, E. S. Saltzman, and P.-Y. Whung (1995), A 340 year record of biogenic sulphur from the Weddell Sea area, Antarctica, *Ann. Glaciol.*, *21*, 169–174.

Rhodes, R. H., N. A. N. Bertler, J. A. Baker, S. B. Sneed, H. Oerter, and K. R. Arrigo (2009), Sea ice variability and primary productivity in the Ross Sea, Antarctica, from methylsulphonate snow record, *Geophys. Res. Lett.*, *36*, L10704, doi:10.1029/2009GL037311.

Slezak, D., A. Brugger, and G. J. Herndl (2001), Impact of solar radiation on the biological removal of dimethylsulfoniopropionate and dimethylsulfide in marine surface waters, *Aquat. Microb. Ecol.*, *25*, 87–97, doi:10.3354/ame025087.

Slezak, D., R. P. Kiene, D. A. Toole, R. Simó, and D. J. Kieber (2007), Effects of solar radiation on the fate of dissoved DMSP and conversion to DMS in seawater, *Aquat. Sci.*, *69*(3), 377–393, doi:10.1007/s00027-007-0896-z.

Stefels, J. (2000), Physiological aspects of the production and conversion of DMSP in marine algae and higher plants, *J. Sea Res.*, *43*, 183–197, doi:10.1016/S1385-1101(00)00030-7.

Stefels, J., and L. Dijkhuizen (1996), Characteristics of DMSP-lyase in *Phaeocystis* sp. (Prymnesiophyceae), *Ecol. Prog. Ser.*, *131*, 307–313, doi:10.3354/meps131307.

Stefels, J., M. Steinke, S. Turner, G. Malin, and S. Belviso (2007), Environmental constraints on the production and removal of the climatically active gas dimethylsulphide (DMS) and implications for ecosystem modelling, *Biogeochemistry*, *83*, 245–275, doi:10.1007/s10533-007-9091-5.

Stefels, J., J. W. H. Dacey, and J. T. M. Elzenga (2009), In vivo DMSP-biosynthesis measurements using stable-isotope incorporation and proton-transfer-reaction mass spectrometry (PTR-MS), *Limnol. Oceanogr. Methods*, *7*, 595–611.

Steinke, M., G. V. Wolfe, and G. O. Kirst (1998), Partial characterisation of dimethylsulfoniopropionate (DMSP) lyase isozymes in 6 strains of *Emiliania huxleyi*, *Mar. Ecol. Prog. Ser.*, *175*(3), 215–225, doi:10.3354/meps175215.

Thomas, D. N., and S. Papadimitriou (2003), Biogeochemistry of sea ice, in *Sea Ice: An Introduction to Its Physics, Biology, Chemistry and Geology*, edited by D. N. Thomas and G. S. Dieckmann, pp. 267–302, Blackwell Sci., Oxford, U. K.

Timco, G. W., and R. M. W. Frederking (1996), A review of sea ice density, *Cold Reg. Sci. Technol.*, *24*, 1–6.

Tison, J.-L., A. Worby, B. Delille, F. Brabant, S. Papadimitriou, D. Thomas, J. de Jong, D. Lannuzel, and C. Haas (2008), Temporal evolution of decaying summer first-year sea ice in the western Weddell Sea, Antarctica, *Deep Sea Res., Part II*, *55*, 975–987, doi:10.1016/j.dsr2.2007.12.021.

Trevena, A. J., and G. B. Jones (2006), Dimethylsulphide and dimethylsulphoniopropionate in Antarctic sea ice and their release during sea ice melting, *Mar. Chem.*, *98*, 210–222, doi:10.1016/j.marchem.2005.09.005.

Trevena, A. J., G. B. Jones, S. W. Wright, and R. L. van den Enden (2003), Profiles of dimethylsulphoniopropionate (DMSP), algal pigments, nutrients and salinity in the fast ice of Prydz Bay, Antarctica, *J. Geophys. Res.*, *108*(C5), 3145, doi:10.1029/2002JC001369.

Turner, S. M., P. D. Nightingale, W. Broadgate, and P. S. Liss (1995), The distribution of dimethyl sulphide and dimethylsulphoniopropionate in Antarctic waters and sea ice, *Deep Sea Res., Part II*, *42*(4–5), 1059–1080.

Welch, K. A., P. A. Mayewski, and S. I. Whitlow (1993), Methanesulfonic acid in coastal Antarctic snow related to sea-ice extent, *Geophys. Res. Lett.*, *20*(6), 443–446.

Wolff, E. W., et al. (2006), Southern Ocean sea-ice extent productivity and iron flux over the past eight glacial cycles, *Nature*, *440*, 491–496.

Yentsch, C. S., and D. Menzel (1963), A method for the determination of phytoplankton chlorophyll and phaeophytine by fluorescence, *Deep Sea Res.*, *10*, 221–231.

Zemmelink, H., L. Houghton, J. W. H. Dacey, A. P. Worby, and P. S. Liss (2005), Emission of dimethylsulfide from Weddell Sea leads, *Geophys. Res. Lett.*, *32*, L23610, doi:10.1029/2005GL024242.

Zemmelink, H., J. W. H. Dacey, L. Houghton, E. J. Hintsa, and P. S. Liss (2008), Dimethylsulfide emissions over the multi-year ice of the western Weddell Sea, *Geophys. Res. Lett.*, *35*, L06603, doi:10.1029/2007GL031847.

F. Brabant and J.-L. Tison, Laboratoire de Glaciologie, Faculté des Sciences, Université Libre de Bruxelles, Av. F.D. Roosevelt 50, CP 160/03, B-1050 Bruxelles, Belgium. (jtison@ulb.ac.be)

I. Dumont, Ecologie des Systèmes Aquatiques, Faculté des Sciences, Université Libre de Bruxelles, Campus de la Plaine CP 221, Bd. du Triomphe, B-1050 Bruxelles, Belgium.

J. Stefels, Laboratory of Plant Physiology, University of Groningen, PO Box 14, NL-9750 AA Haren, Netherlands.